Astron. Astrophys. 355, 381–393 (2000)

ASTRONOMY AND ASTROPHYSICS

Convective overshooting on the Sun: radiative effects

M. Kiefer[1,⋆], **U. Grabowski**[1,⋆], **W. Mattig**[1], **and M. Stix**[1]

Kiepenheuer-Institut für Sonnenphysik, Schöneckstrasse 6, 79104 Freiburg, Germany (kiefer@kis.uni-freiburg.de, stix@kis.uni-freiburg.de)

Received 26 August 1999 / Accepted 4 January 2000

Abstract. We calculate solar models with convective overshooting at the top and at the base of the outer convection zone, and test the models by comparing their eigenfrequencies to the observed solar p-mode frequencies. Radiative temperature relaxation is included in form of a characteristic time that describes both optically thick and thin cases, and a modified mixing-length formalism is used, with gas parcels traveling varying path lengths. These modifications to the common mixing-length theory generally change the efficiency of the convective energy transport, and therefore the stratification at and immediately below the surface of the Sun. Radiative relaxation lowers the convective efficiency and so leads to a steeper temperature gradient, with the consequence that the temperature becomes somewhat larger in the near-surface layer, but slightly lower in the upper convection zone; due to the latter effect there is a negative correction to eigenfrequencies above $\approx 2\,\mathrm{mHz}$. The effect of convective parcels with varying path lengths is opposite.

In the solar interior, radiative relaxation is in the diffusion limit and therefore has no immediate effect at the base of the convection zone. However, the larger mixing-length to scale-height ratio caused by the near-surface effect leads to farther overshooting at the base. The effect of the multiple-path models is in the same direction. For most of our models the extent of the overshooting is larger than permitted by the helioseismic constraint of ≈ 0.1 pressure scale heights, but for some models it is marginal.

At the surface the efficient optically thin radiative relaxation smoothes the temperature gradient. Both the radiation and the multiple-path effects lead to more extended overshooting. The models reach ≈ 200 km of overshooting, with temperature fluctuations of up to several hundred Kelvin. We compare the results with spectroscopic investigations, and with recent three-dimensional hydrodynamic numerical simulations.

A general result is that mixing-length theory appears unable to reproduce in detail the properties of solar convection that are directly observed at the surface or inferred by helioseismology. The improvements based on even sophisticated modifications remain limited.

Key words: convection – Sun: oscillations – Sun: photosphere

1. Introduction

The outer convection zone of the Sun occupies $\approx 29\%$ of the radius, but the largest uncertainty about its thermal and dynamic state is related only to a relatively thin layer of a few pressure scale heights near the surface. Close to the surface the deviation of the mean temperature from the adiabatic stratification is the largest; here the diverse descriptions of the convective energy transport lead to significant differences of the solar model structure and hence have significant consequences to the frequencies of the solar p-mode oscillations (Christensen-Dalsgaard 1997). For example, the modified mixing-length formalism of Canuto & Mazzitelli (1991, 1992) and Canuto et al. (1996) yields solar models with improved eigenfrequencies (Paternò et al. 1993), as compared to the standard mixing-length model described by Böhm-Vitense (1958).

At the solar surface the transition to the optically thin state constitutes a particular complication for the description of the convection. This is the first subject of the present contribution. With the help of an expression first derived by Spiegel (1957) we shall formulate the radiative temperature relaxation of a convective parcel, in a way that is valid in the optically thin as well as in the optically thick case. Henyey et al. (1965) and Ulrich (1970a) have considered a similar transition, based on an interpolation formula that models Spiegel's result. Nevertheless we think that it is worth to reconsider the problem: our treatment is simpler and more transparent – Eqs. (8) and (9) below –, and it goes further in that we test the ensuing solar models by calculating their eigenfrequencies of oscillation. It will be seen that significant corrections to the frequencies can be obtained.

Unsöld (1930) first attributed the granulation seen in the stably stratified solar atmosphere to a convective instability immediately underneath the visible surface. Since then, such convective *overshooting* has been investigated spectroscopically with increasing detail; a brief review will be given in Sect. 5.3 below. Theoretical efforts in-

Send offprint requests to: M. Stix (stix@kis.uni-freiburg.de)

⋆ *Present address:* Institut für Meteorologie und Klimaforschung, Forschungszentrum Karlsruhe GmbH, Postfach 3640, 76021 Karlsruhe, Germany

Table 1. Parameters of the reference solar model, based on mixing-length models according to Böhm-Vitense (STD and MLT1) and Canuto & Mazzitelli (CM..); z^* is the distance to the upper border of the convection zone, and H_P^* is the pressure scale height at that level.

Model	$l_{\rm mix}$	α	A	B	C	D
STD	αH_P	1.6704	0.036	8.66	-0.139	1.96
MLT1	$z^* + \alpha H_P^*$	1.3498	0.012	7.85	-0.101	1.64
CM30	αH_P	0.8597	0.076	8.82	-0.252	1.85
CM31	$z^* + \alpha H_P^*$	0.4404	0.057	8.79	-0.182	2.01
CM40	αH_P	0.7409	0.089	8.82	-0.294	1.85
CM41	$z^* + \alpha H_P^*$	0.2410	0.069	8.79	-0.214	2.02

clude diverse "non-local" versions of the mixing-length theory (Spiegel 1963, Ulrich 1970a, Ulrich 1970b, Ulrich 1976) and, more recently, numerical hydrodynamic simulations (Kim & Chan 1998, Stein & Nordlund 1998 who give earlier references). With "non-local" one usually means (as we do in this paper) that the variation of diverse quantities along the path of a convecting parcel is taken into account when its temperature excess and velocity are calculated. As the second subject of this contribution, we shall calculate convective overshooting in solar models. The calculation will be based on the adiabatic non-local mixing-length formalism of Shaviv & Salpeter (1973), with the modification that the convective parcels will be allowed to travel paths of variable length and that radiative temperature relaxation will be included. Applications to both the upper and lower boundary regions of the solar convection zone will be made.

2. The reference model

In this section we specify the standard solar model that serves as a reference for all our results reported in this paper. This model is named STD; it is evolved from a homogeneous star of $1\,m_\odot$ (zero-age main sequence) in 25 time steps to the age of 4.6×10^9 years. We use the MHD equation of state (Hummer & Mihalas 1988, Mihalas et al. 1988) and a combination of the OPAL95 opacity table (Iglesias & Rogers 1996) with a low-temperature table of Alexander & Ferguson (1994). For the abundance of heavy elements we take the mass fraction $Z = 0.02$; the original mass fraction of helium, Y_0, is adjusted – together with a mixing-length parameter α – in order that the latest model of the sequence has the luminosity and the radius of the present Sun. Element diffusion during the evolution has been neglected. This is justified because we only want to compare solar models with different prescriptions of convection.

2.1. Mixing-length formalisms

In our reference model STD convective energy transport is calculated by means of the mixing-length theory of Böhm-Vitense (1958; see e.g. Stix 1989), where the mixing length is a multiple of the pressure scale height, $l_{\rm mix} = \alpha H_P$, with constant α. For comparison we also calculate modified standard models. The first, MLT1, uses $l_{\rm mix} = z^* + \alpha H_P^*$, where z^* is the distance to the upper border of the convection zone, H_P^* is the pressure scale height at that level, and α is again a (smaller) constant. Four other models employ the formalisms described by Canuto & Mazzitelli (1991) – models CM30 and CM31 –, and by Canuto et al. (1996) – models CM40 and CM41 –, either with $l_{\rm mix} = \alpha H_P$ or with $l_{\rm mix} = z^* + \alpha H_P^*$ as proposed by Canuto & Mazzitelli (1992). In Table 1 we list the adjusted values of α and of the luminosity and radius variations with respect to α and Y_0,

$$A = \left(\frac{\partial L/L_\odot}{\partial \alpha}\right)_{Y_0} \qquad B = \left(\frac{\partial L/L_\odot}{\partial Y_0}\right)_{\alpha} \tag{1}$$

$$C = \left(\frac{\partial r/r_\odot}{\partial \alpha}\right)_{Y_0} \qquad D = \left(\frac{\partial r/r_\odot}{\partial Y_0}\right)_{\alpha} . \tag{2}$$

All these models yield the same $Y_0 = 0.2785$, the same depth of the convection zone, $r_{\rm CZ}/r_\odot = 0.724$ with temperature $T(r_{\rm CZ}) = 2.13\times10^6$ K, and the same parameters at the center, namely $T_{\rm c} = 1.558\times10^7$ K, $\rho_{\rm c} = 1.495\times10^5$ kg/m^3, and $P_{\rm c} = 2.297\times10^{16}$ Pa. Models with $l_{\rm mix} = z^*$, with no adjustable mixing-length parameter, have also been calculated; but such models have large deviations of their radius and luminosity from the solar values.

The main difference between the 6 models of Table 1 lies in the temperature stratification in a shallow layer immediately below the solar surface. The temperature gradient ∇ is increased in that layer (Fig. 1a), and the temperature itself is slightly larger near the surface (Fig. 1b), and slightly lower in the upper parts of the convection zone (not shown). As a consequence, the eigenfrequencies of the p-mode oscillations in the range above ≈ 2 mHz decrease slightly, a result already obtained by Paternò et al. (1993) and confirmed by our own calculations. In a perturbation approach this frequency change can be understood in terms of an integral over the variation of the inverse sound speed in the depth range where the stratification is modified (Kiefer et al. 1996 e.g.). The decrease constitutes an improvement of the theoretical frequencies which are somewhat too large when the ordinary mixing-length model is used, see Fig. 2.

2.2. Envelope models

In the present contribution we are especially interested in the outer convection zone of the Sun. For the diverse models we therefore integrate the basic equations only in an envelope, which may extend far into the radiative interior, but not into the core where nuclear energy is generated. In principle, envelope models are completely defined by the boundary conditions at the surface, and therefore would not allow for the adjustment of Y_0 and α by calibrating the luminosity and the radius. Nevertheless, we determine Y_0 and α values for each individual model by a comparison (and iterative adjustment) of the temperature and pressure at an arbitrarily chosen depth within the envelope to the corresponding values of the reference model STD; for

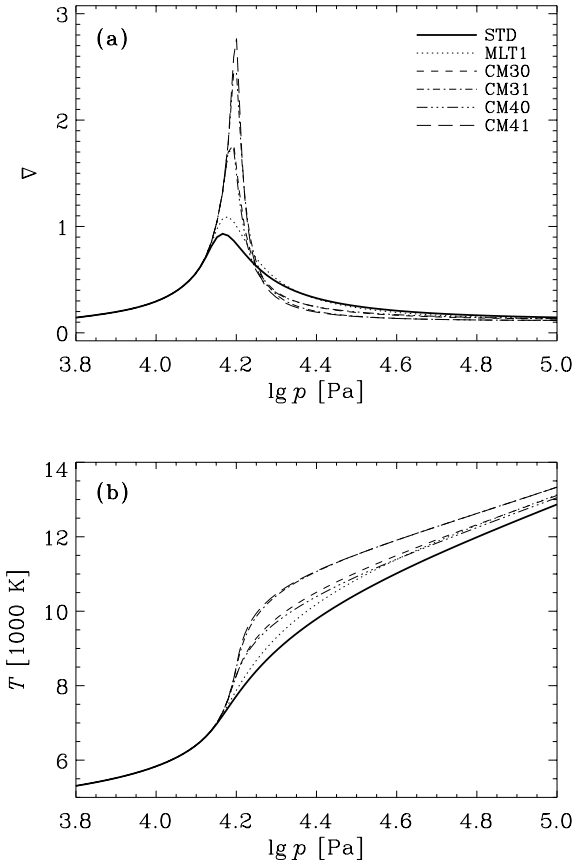

Fig. 1a and b. Temperature gradient ∇ (**a**) and temperature (**b**) in the uppermost part of the convection zone for diverse forms of the mixing-length theory.

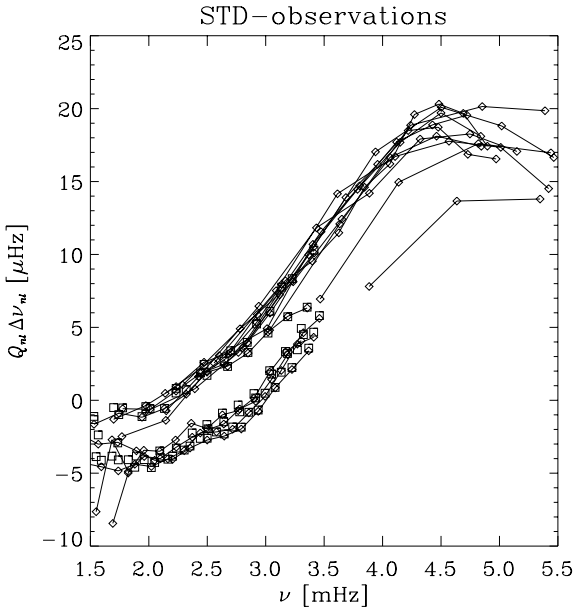

Fig. 2. Difference between oscillation frequencies of model STD and observed frequencies, for harmonic degrees $l = 0$, 5, 10, 20, 40, 60, 80, 100, 150, 200, 250, 300, 350, 400, 500, 600, 800, 1000. *Squares* denote data from Tomczyk for $l < 100$ (pers. comm.), *diamonds* denote data from Libbrecht et al. (1990) ($l \leq 80$) and from Bachmann et al. (1995) ($l \geq 100$). The weighting Q_{nl} is taken from Fig. 5.16 of Christensen-Dalsgaard (1994).

technical reasons $r = 0.78989 r_\odot$ is chosen for this comparison. The calculations are done on a grid with points equidistant in $\ln P$. A total of 2000 grid points between the upper and lower boundary of the convection zone is chosen.

To each envelope model an atmosphere is calculated by means of a linear relation between T^4 and τ as obtained in the Eddington approximation, and is fitted at optical depth $\tau = 2/3$ with continuous pressure and temperature. For the models with overshooting convection at the upper edge of the convection zone this complicates the calculation since the overshooting motion extends to levels where $\tau < 2/3$ (the Schwarzschild boundary lies ≈ 30 km below that level). The envelope model is therefore calculated upwards until the end of the overshooting, and an additional iteration ensures a continuous pressure stratification at that level. The details of the model calculation have been described by Kiefer (1999). Test calculations show that the envelope models described here and models calculated in a consistent manner into the solar center differ so little that there are no consequences as to the conclusions drawn in this paper.

2.3. Adiabatic oscillations

As a test to our diverse solar models we calculate the eigenfrequencies of p-mode oscillations. The numerical scheme used for these calculations is that of Grabowski (1996), based on a first-order Newton-Raphson iteration. The scheme employs a discretization of fourth order on a variable grid. For the same number of grid points, the convergence is twice as rapid as with classical first or second order approaches. With 3000 points over the whole star the frequencies are stable to all significant digits in the full frequency range. The price to pay are rather accurate initial eigenfunction guesses.

Attempts to use central fourth-order differences led to a numerically unstable system, so we have chosen an off-centered, asymmetric scheme where the equations are solved in between the grid points. The grid is not the same as that used in the solar model calculation, therefore interpolation was necessary. The coefficients of the differential equations are calculated at the grid points with a fifth-order interpolation. The grid points themselves can be distributed according to a grid function with an integral formulation developed by Thompson et al. (1985), with a grid-density smoothing function given in Dorfi et al. (1987). The grid-density function is chosen to allow for high resolution of the upper layers of the Sun which mainly determine the frequency spacing, as well as a dense core spacing to give better frequencies for low-degree, high-order oscillation modes. The higher grid density in the core also results in significantly enhanced eigenfunctions near the center. The resulting five-block, band-diagonal matrix is solved by complete Gauss-Jordan reduction of the diagonal blocks and subsequent Gauss elimination to upper triangular form with back-substitution to the final solution. This method only requires storage of the up-

per block bands, and is still the fastest known algorithm for this type of problem.

Standard models of the Sun often have slightly too large eigenfrequencies of oscillation, in comparison to the observed frequencies of the Sun; the excess increases with increasing harmonic degree l and with increasing frequency ν. Our model STD is no exception in this respect. Fig. 2 shows the difference between the frequencies of model STD and observed values. For our comparison we took data from Tomczyk for $l < 100$ (Tomczyk, pers. comm.) obtained with the LOWL-instrument (Tomczyk et al. 1995), data from Libbrecht et al. (1990) for $l \leq 80$ and data from Bachmann et al. (1995) for $l \geq 100$. The dependence on degree l is essentially accounted for by multiplication with the 'mode mass' Q_{nl} (Christensen-Dalsgaard 1994), but the dependence on ν is marked; the excess reaches $\approx 20\,\mu$Hz at $\nu = 4.5$ mHz.

A part of these deviations might be explained by the following effects: We calculate adiabatic oscillations but it is known that non-adiabatic effects can have a non-negligible influence on some modes and their frequencies, see e.g. Guenther (1994), Rosenthal et al. (1995). Element diffusion leads to a solar structure different to ours. Therefore changes to the eigenfrequencies occur (Guenther 1994). The dynamic or turbulent pressure alters the frequencies too; it can reach several percent of the gas pressure in mixing-length models, and according to numerical simulations of the upper convection zone it may even reach up to 15% (Rosenthal et al. 1999). The oscillations are calculated for a homogeneous outer convection zone. Structuring of this region by the fluctuations in sound velocity and convective velocity leads to frequency changes (Zhugzhda & Stix 1994, Stix & Zhugzhda 1998). Again we stress that we only want to do relative comparisons between models and therefore neglect all above effects because we expect them to show almost the same impact for all of our diverse models.

3. Modifications of the mixing-length theory

3.1. Radiative relaxation

Radiative energy exchange of a gas parcel with its environment reduces the convective transport of energy. In its common form mixing-length theory takes account of this effect by replacing the adiabatic temperature gradient ∇ by a slightly larger gradient ∇' that is necessary to compensate for the radiative loss. The loss itself is estimated in an approximation that is valid in the optically thick case.

In this contribution we prefer a formalism that can be used for the optically thin as well as for the optically thick case. We consider a characteristic time of radiative relaxation, τ_q, as was first introduced by Spiegel (1957). In such an approximation, and with $\beta = (\mathrm{d}T/\mathrm{d}r)_{\mathrm{ad}} - \mathrm{d}T/\mathrm{d}r$ the temperature excess ΔT of a parcel is governed by

$$\frac{\mathrm{d}\,\Delta T}{\mathrm{d}\,t} = \beta w - \frac{\Delta T}{\tau_q}\,, \tag{3}$$

where w is the vertical velocity. If the parcel is in pressure equilibrium with its environment, then $\Delta\rho/\rho = -\delta\,\Delta T/T$, where $\delta = -(\partial\,\ln\rho/\partial\,\ln T)_P$. Thus, a buoyancy force accelerates the parcel according to

$$\frac{\mathrm{d}\,w}{\mathrm{d}\,t} = g\delta\frac{\Delta T}{T}\,. \tag{4}$$

If both ΔT and w vary as $\exp(\sigma t)$ one finds

$$\sigma_{1,2} = -\frac{1}{2\tau_q} \pm \sqrt{\frac{1}{4\tau_q^2} + \frac{\beta g\delta}{T}}\,. \tag{5}$$

In the adiabatic case, $\tau_q \to \infty$, this yields either exponential growth of the parcels excursion, or the well-known oscillation with the Brunt-Väisälä frequency $N = \sqrt{-\beta g\delta/T}$, depending on the sign of β. In the opposite, radiatively dominated, case ΔT decays with the time constant τ_q.

As in the common form of the mixing-length theory, we seek a solution (ΔT, w) of Eqs. (3) and (4), take

$$F_{\mathrm{conv}} = \rho c_P w\Delta T\,, \qquad F_{\mathrm{rad}} = \frac{16\sigma T^4}{3\kappa\rho H_P}\nabla, \tag{6}$$

and use the equation for the total flux,

$$F_{\mathrm{conv}} + F_{\mathrm{rad}} = L/4\pi r^2. \tag{7}$$

Both F_{conv} and F_{rad} depend on the temperature gradient ∇; therefore (7) can be solved for ∇.

The solution (ΔT, w) is obtained as follows. Eq. (3) is divided by w, and (4) is multiplied by w. This yields

$$\frac{\mathrm{d}\,\Delta T}{\mathrm{d}\ln P} = -\beta H_P + \frac{H_P}{w\tau_q}\Delta T\,, \tag{8}$$

$$\frac{\mathrm{d}\,w^2}{\mathrm{d}\ln P} = -g\delta\frac{\Delta T}{T}H_P\,, \tag{9}$$

where, in addition, $\ln P$ has been chosen as independent variable, and – again following common mixing-length theory – a factor 1/2 has been added on the right-hand side of (4) to account for the loss by friction. For brevity, we introduce $x = \ln P$ and obtain

$$\frac{\mathrm{d}\,\Delta T}{\mathrm{d}\,x} = a + b\frac{\Delta T}{w}\,, \qquad \frac{\mathrm{d}\,w}{\mathrm{d}\,x} = \frac{c}{2}\frac{\Delta T}{w}\,, \tag{10}$$

where

$$a = -\beta H_P\,, \qquad b = \frac{H_P}{\tau_q}\,, \qquad c = -\frac{g\delta H_P}{T}\,. \tag{11}$$

In our model the parcels start at level x_{s}, therefore

$$\Delta T(x_{\mathrm{s}}) = w(x_{\mathrm{s}}) = 0\,. \tag{12}$$

In the standard approximation the coefficients a, b, and c are treated as constants along the path of a convective element. The solution to Eqs. (10) that obeys the boundary conditions (12) is then

$$\Delta T = \left(a + \frac{b}{c}\left(b - \sqrt{b^2 + 2ac}\right)\right)(x - x_{\mathrm{s}})\,, \tag{13}$$

$$w = \frac{1}{2}\left(b - \sqrt{b^2 + 2ac}\right)(x - x_{\mathrm{s}})\,. \tag{14}$$

Table 2. Solar models calculated with the modified mixing-length theory

Model	$l_{\rm mix}$	$l_{\rm opt}/l_{\rm mix}$	Y_0	α	$r_{\rm CZ}/r_\odot$
STD	αH_P	8/9	0.2785	1.6704	0.7242
MLT1	$z^* + \alpha H_P^*$	8/9	0.2784	1.3498	0.7241
SP1	αH_P	1	0.2785	1.6772	0.7242
SP4	$z^* + \alpha H_P^*$	1	0.2784	1.3650	0.7241
SP2	αH_P	1/2	0.2785	1.8287	0.7242
SP5	$z^* + \alpha H_P^*$	1/2	0.2784	1.6986	0.7241
SP3	αH_P	1/4	0.2785	2.0978	0.7242
SP6	$z^* + \alpha H_P^*$	1/4	0.2784	2.2826	0.7240

The sign of the square root has been chosen such that in the limit $b \to \infty$, where the radiative relaxation is very fast, the temperature perturbation vanishes. In the adiabatic limit, $b \to 0$, we recover the ordinary expressions for ΔT and w of the mixing-length theory (with ∇' replaced by $\nabla_{\rm ad}$).

For the general case we must now specify τ_q. With $l_{\rm opt}$ we denote the distance over which ΔT changes by a substantial fraction, and with $\lambda_{\rm opt}$ the optical depth $\kappa\rho l_{\rm opt}$. The relaxation time derived by Spiegel (1957) is then

$$\tau_q = \frac{c_V}{16\kappa\sigma T^3(1 - \lambda_{\rm opt}\arctan(1/\lambda_{\rm opt}))} \,. \qquad (15)$$

In the optically thick case, $\lambda_{\rm opt} \gg 1$, an expansion of the arctan function leads to the diffusion approximation, where $\tau_q \propto \lambda_{\rm opt}^2$. On the other hand, $\tau_q = c_V/16\kappa\sigma T^3$ becomes independent of $\lambda_{\rm opt}$ in the optically thin case, where $\lambda_{\rm opt} \ll 1$.

We have defined the dimensionless parameter $\lambda_{\rm opt}$ as the ratio of the length scale $l_{\rm opt}$ of temperature variation in the convective parcel to the photon mean-free-path, $1/\kappa\rho$. The scale $l_{\rm opt}$ should be related to the mixing length $l_{\rm mix}$; in fact $l_{\rm opt}/l_{\rm mix} = 8/9$ in the common form of mixing-length theory (Stix 1989 for a presentation). Table 2 lists a number of models that have been calculated with the radiative relaxation as described in this section, for diverse values of $l_{\rm opt}/l_{\rm mix}$. Except for the parameter α, there is little change in the model parameters. However, there is a marked influence on the stratification of the near-surface layer (Fig. 3), rather similar to the effect seen in the CM models above (Fig. 1). As in those models, the efficiency of the convective energy transport is diminished in the modified theory; but this time the reason is the transition from the optically thick solar interior to the optically thin atmosphere. Smaller values of $l_{\rm opt}$ shift this transition into somewhat greater depth. Deeper in the convection zone the temperature is slightly reduced in comparison to the reference model, although there is virtually no change right at the base of the convection zone, cf. the values $r_{\rm CZ}/r_\odot$ listed in the table.

As might be expected, the similar modification of the thermal structure causes changes of the oscillation frequencies similar to those of the CM models above. The frequency changes of four models are shown in Fig. 4. A comparison with Fig. 2 indicates that the theoretical frequencies are improved. Both the transition to the optically-thin radiative relaxation and the modified mixing length $z^* + \alpha H_P^*$ contribute to this effect.

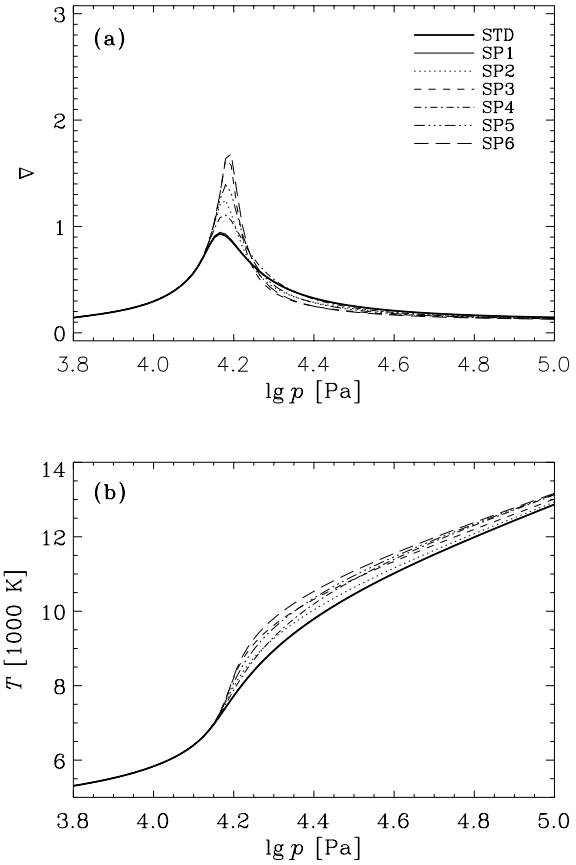

Fig. 3. Temperature gradient ∇ (**a**) and temperature (**b**) in the uppermost part of the convection zone for models based on local mixing-length theory with modified radiative relaxation (cf. Table 2).

3.2. A multi-parcel model

We now include our scheme of radiative relaxation into a "non-local" version of the mixing-length formalism. Shaviv & Salpeter (1973) first employed a "non-local" extension to standard MLT. They assumed adiabatic movement of the convective parcels. This prescription was implemented into solar models by Pidatella & Stix (1986) and Skaley & Stix (1991). In contrast to this, our present approach includes dissipation by radiative effects. Therefore it does not appear feasible to express ΔT and w^2 in the form of definite integrals over the mixing length. Instead the two coupled equations (10) have been integrated numerically. The common feature of this numerical solution of differential equations and the earlier evaluation of integrals (and in fact of the local mixing-length formalism) is that ΔT and w contain the unknown temperature gradient ∇ at the specific level under consideration (the end point of the parcel's path). The equation for the total energy flux, Eq. (7), is then used to determine ∇.

The numerical scheme of solving the two coupled equations can easily be extended to a model in which several parcels, each starting at a different distance from the level where ΔT and w are to be evaluated, contribute to the convective energy transport. Such a multi-parcel model was first proposed by Renzini (1987).

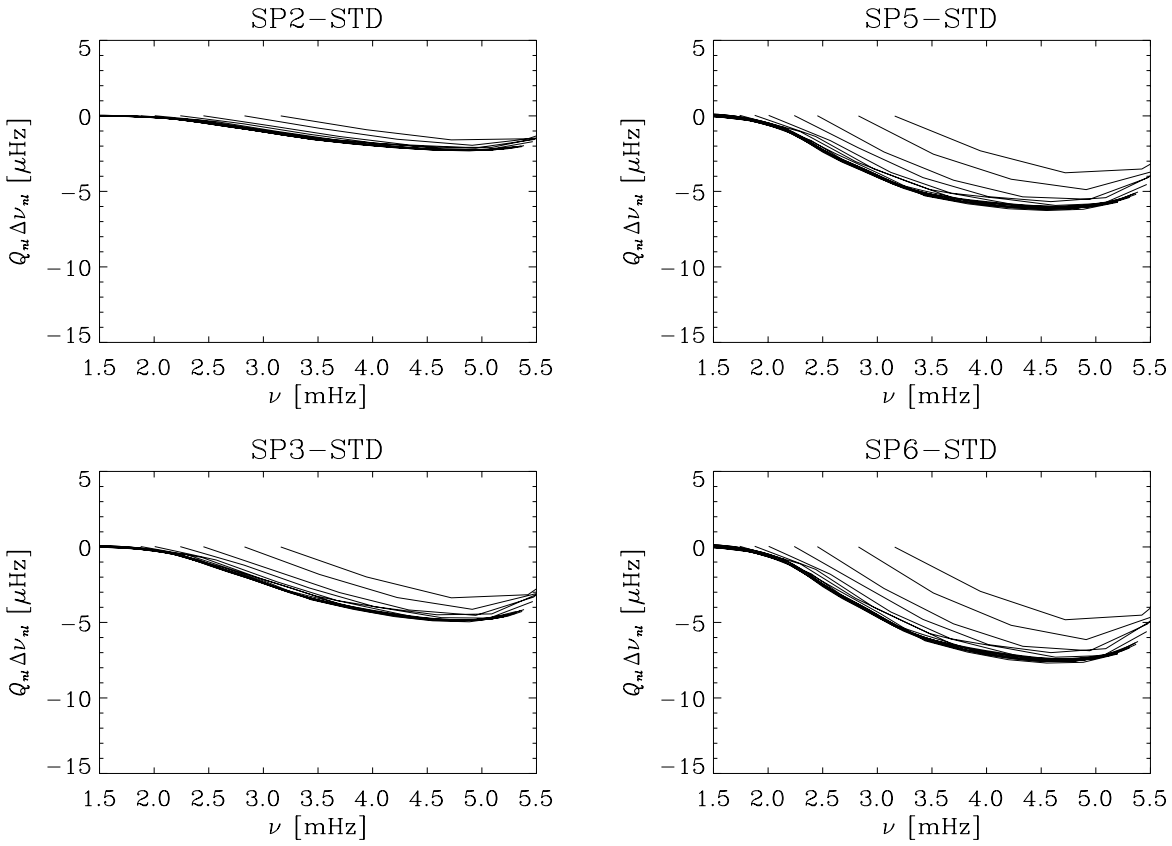

Fig. 4. Frequency changes of four local mixing-length models with modified radiative relaxation (cf. Table 2), as compared to model STD. The changes are calculated for the same degrees $l = 0 \ldots 1000$ as in Fig. 2, in ascending order of the curves, and with weights Q_{nl} as in Fig. 2.

We distribute the start positions evenly over the mixing length. That is, the mth of M parcels starts at

$$x_{\mathrm{s},m} = x - m\alpha/(M+1)\ , \tag{16}$$

where again $x = \ln P$, and where the case of *descending* parcels has been considered, to be specific. This distribution is chosen such that the mean $\langle x - x_{\mathrm{s},m}\rangle$ is $\alpha/2$, as with the assumption underlying the common local formalism. Each parcel starts from rest and with the temperature of its environment; therefore the boundary conditions (12) are replaced by

$$\Delta T_m(x_{\mathrm{s},m}) = w_m(x_{\mathrm{s},m}) = 0\ . \tag{17}$$

We assume that each parcel makes an independent contribution to the convective transport of energy, so that

$$F_{\mathrm{conv}} = c_P\rho\frac{1}{M}\sum_{m=1}^{M} w_m\Delta T_m\ . \tag{18}$$

The computational scheme of the "non-local" models has been explained in more detail by Kiefer (1999). We shall now consider applications of both the optically-thick/thin radiative relaxation and the multi-parcel model to the boundary regions of the solar convection zone.

4. Results for the base of the convection zone

Convective overshooting is a consequence of the "non-local" treatment. Our models with overshooting at the base of the solar convection zone are summarized in Table 3. In all these models the standard mixing-length formalism is replaced by the "non-local" calculation at a certain level inside the convection zone, near $r = 0.86\,r_\odot$, and downward traveling parcels of gas are considered. The transition is such that the convective energy flux F_{conv} is continuous, and the ensuing temperature gradient ∇ has been smoothed over an interval Δx of about 1 pressure scale height. Table 3 shows that the model calibration always yields nearly the same Y_0 but, since the efficiency of convection differs in the diverse models, different values of α are obtained. Generally, less efficient, e.g. non-adiabatic, convection requires a larger α, so that the product $w\Delta T$ remains the same.

Table 3 lists the level r_{CZ} where $w = 0$, and the thicknesses $d_{\Delta\nabla<0}$ and $d_{F_{\mathrm{conv}}<0}$ of the layers with reversed superadiabaticity and convective flux. The latter, $d_{F_{\mathrm{conv}}<0}$, is the *depth of the layer of overshooting convection*. We notice that the non-adiabatic treatment as well as an increasing number of parcels and a decreasing length l_{opt} lead to deeper convection zone models, and to increased values of $d_{\Delta\nabla<0}$ and $d_{F_{\mathrm{conv}}<0}$. To a smaller part, the reason lies in the overshoot layer itself, where the braking action of a positive temperature excess ΔT is diminished by radiative relaxation. The main reason, however, is

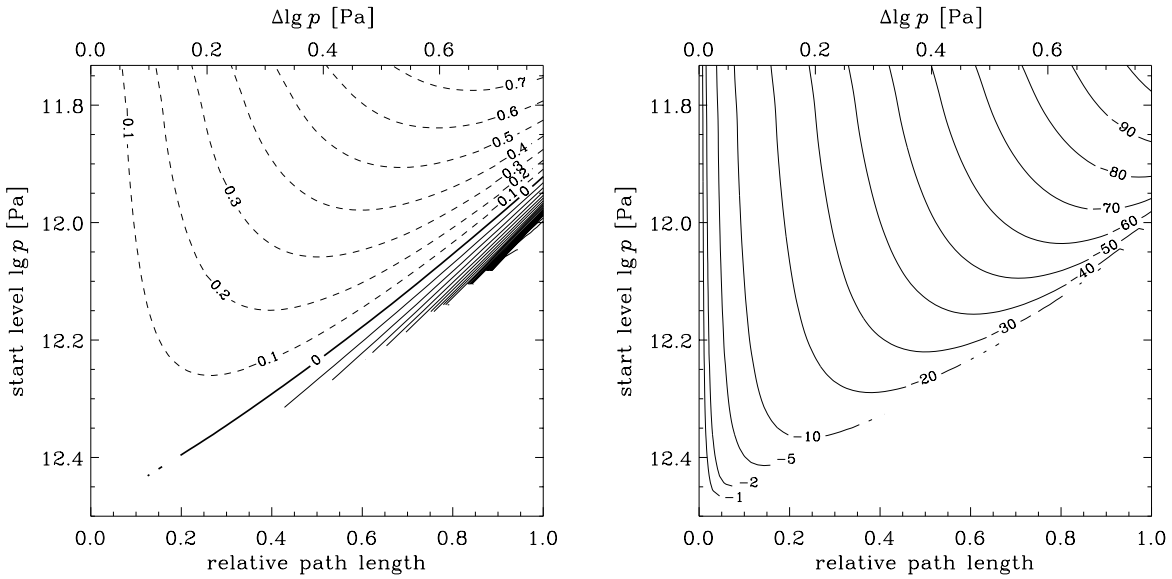

Fig. 5. Temperature excess ΔT (*left*) and vertical velocity w (*right*) of gas parcels along their path towards the base of the convection zone, for a 32-parcel model with $l_{\rm opt}/l_{\rm mix} = 1$. The ordinate plus the upper abscissa gives the actual parcel position, the lower abscissa gives the path fraction of the total range of integration. Iso-ΔT curves are labeled in K, *solid* positive, *dashed* negative. Iso-w curves are labeled in m/s.

Table 3. Solar models based on non-local mixing-length theory in the deeper part of the convection zone, including non-adiabatic and multi-parcel calculations. The layer widths $d_{\Delta\nabla<0}$ and $d_{F_{\rm conv}<0}$ are in km

a) adiabatic convection ($b = 0$). $Y_0 = 0.2784$, $\alpha = 1.5505$

M	$r_{\rm CZ}/r_\odot$	$d_{\Delta\nabla<0}$	$d_{F_{\rm conv}<0}$
1	0.7146	27291	6197
2	0.7102	31144	9262
4	0.7080	33166	10806
8	0.7069	34661	11581
16	0.7069	35569	11581

b) non-adiabatic convection. $Y_0 = 0.2785$, $\alpha = 1.6764$

M	$r_{\rm CZ}/r_\odot$	$d_{\Delta\nabla<0}$	$d_{F_{\rm conv}<0}$
1	0.7136	26725	6959
2	0.7103	31810	9261
4	0.7069	35511	11579
8	0.7058	37728	12356
16	0.7058	37996	12356
32	0.7058	38102	12356

c) dependence on $l_{\rm opt}$. $Y_0 = 0.2785 \ldots 0.2788$

M	$l_{\rm opt}/l_{\rm mix}$	α	$r_{\rm CZ}/r_\odot$	$d_{\Delta\nabla<0}$	$d_{F_{\rm conv}<0}$
1	1	1.6764	0.7136	26725	6959
1	0.5	1.8276	0.7125	25051	7723
1	0.25	2.0958	0.7114	29858	8488
32	1	1.6764	0.7058	38102	12356
32	0.5	1.8276	0.7036	41617	13912
32	0.25	2.0958	0.7002	47142	16262

the larger α value that is required for the model calibration; this calibration is mostly influenced by the near-surface layer where – due to the transition to the optically thin regime – the non-adiabatic behavior is more severe. With larger α, the parcels have a longer path available to gain kinetic energy and thus may penetrate further.

At the base of the convection zone, $r = r_{\rm CZ}$, all our models have a rather discontinuous transition from the nearly adiabatic temperature gradient to the radiative gradient. For a stratification of this type helioseismology allows only for overshooting over $\approx 7\%$ of a pressure scale height according to Monteiro et al. (1994), cf. also Christensen-Dalsgaard et al. (1995) or over $\approx 10\%$ of H_P according to Basu et al. (1994). The models described here fail in this respect: the least overshooting that we obtain is 11% of H_P, or $\approx$ 6200 km. This is less than what has been found in earlier calculations – 26 to 53% by Skaley & Stix (1991), or 13 to 19% by Stix & Kiefer (1997) – but perhaps indicates that some essential ingredient to the model is still missing, or even that the present approach to model the overshoot is entirely inadequate.

The increase of $d_{F_{\rm conv}<0}$ with decreasing $l_{\rm opt}/l_{\rm mix}$ (Table 3c) in particular illustrates the effect of the near-surface layer upon the deep part of the convection zone: the length $l_{\rm opt}$ matters only at the surface where the optical depth becomes small, but not in the interior. Nevertheless the parameters $r_{\rm CZ}$, $d_{\Delta\nabla<0}$, and $d_{F_{\rm conv}<0}$ clearly depend on $l_{\rm opt}/l_{\rm mix}$. A mixing-length parameter α that varies with depth might change the situation, but we refrain from such a modification that would add another arbitrariness to the already unpopular mixing-length theory.

The variation of ΔT and w of a convective parcel along its path is shown in Fig. 5. Each path is represented by a horizontal line through the starting position (ordinate); the actual position is the sum of that value and the $\Delta \lg P$ value at the upper abscissa. Only parcels starting above the level where $\lg P \approx 12.0$ reach the full length of the integration range. On their way they pass through the level $\lg P \approx 12.47$ where $\nabla = \nabla_{\rm ad}$ and from

Table 4. Solar models based on non-local mixing-length theory in the upper part of the convection zone, including non-adiabatic and multi-parcel calculations. The levels $h_{\rm cc}$, $h_{F_{\rm conv}=0}$, and $h_{w=0}$ are in km

a) dependence on the form of radiative relaxation

Model	M	rad. rel.	α	$h_{\rm cc}$	$h_{F_{\rm conv}=0}$	$h_{w=0}$
11a	1	adiabatic	1.5914	-24.1	39.4	52.9
15a	1	diffusion	1.7531	-1.5	19.1	84.5
30	1	Eq. (15)	1.7508	-2.2	21.1	75.3
13	32	adiabatic	1.6328	-39.2	90.9	119.2
17	32	diffusion	1.8534	-11.1	39.0	183.9
35	32	Eq. (15)	1.8482	-12.0	46.6	161.8

b) dependence on parcel number M; models based on Eq. (15)

Model	M	α	$h_{\rm cc}$	$h_{F_{\rm conv}=0}$	$h_{w=0}$
30	1	1.7508	-2.2	21.1	75.3
31a	2	1.7898	-5.9	35.9	105.3
32a	4	1.8166	-9.0	41.4	129.4
33	8	1.8338	-10.6	44.4	145.6
34	16	1.8433	-11.5	45.9	155.6
35	32	1.8482	-12.0	46.6	161.8

c) dependence on $l_{\rm opt}/l_{\rm mix}$; models based on Eq. (15)

Model	M	$l_{\rm opt}/l_{\rm mix}$	α	$h_{\rm cc}$	$h_{F_{\rm conv}=0}$	$h_{w=0}$
30	1	1	1.7508	-2.2	21.1	75.3
90	1	0.5	1.9653	2.3	14.0	87.1
91	1	0.25	2.3016	2.9	9.0	102.5
35	32	1	1.8482	-12.0	46.6	161.8
93a	32	0.5	2.0813	0.3	26.0	184.9
94	32	0.25	2.4255	2.7	13.5	216.5

where on their temperature excess ΔT becomes less negative (and finally positive if the start was below $\lg P \approx 11.9$). The magnitude $|w|$ of the velocity has its maximum at the sign reversal of ΔT. Parcels starting from below $\lg P \approx 12.0$ are braked down to $w = 0$ even before the interval of integration ends.

5. Results for the solar surface

5.1. Model calculations

At the solar surface the transition occurs from the optically thick to the optically thin state, which is why radiative relaxation has much more influence on convective overshooting at the surface than at the base of the convection zone: the radiative relaxation time τ_q becomes much smaller than the advection time scale $l_{\rm mix}/w$. In order to demonstrate the essential effect we first show, in Table 4a, models with diverse descriptions of the radiative exchange, namely adiabatic models, models based on the diffusion approximation, and models based on Eq. (15) above. Again the non-adiabatic models have a smaller efficiency of their convective energy transport and therefore need larger α values for compensation.

Three characteristic levels mark the path of a convection parcel; these levels are listed in Table 4. At $h_{\rm cc}$ the sign of $\nabla - \nabla_{\rm ad}$ reverses. Above this level all parcels expand and therefore cool, either adiabatically or – in the non-adiabatic models – even more so by expansion *and* radiative relaxation. The layer between $h_{\rm cc}$ and $h_{F_{\rm conv}=0}$ (where $\Delta T = 0$) is thus shallower in non-adiabatic models. Once $\Delta T = 0$ is reached, at level $h_{F_{\rm conv}=0}$, the parcels are driven further by their remaining kinetic energy. Above $h_{F_{\rm conv}=0}$ the cooling due to expansion is opposed by re-heating through radiative relaxation. Hence the non-adiabatic models have less net cooling and less braking of their parcels by (negative) buoyancy. The level $h_{w=0}$ where the parcels come to rest and the convection zone ends lies higher in the atmosphere for these models. Since radiative relaxation in the diffusion approximation is slightly faster than in the models based on Spiegel's formula, Eq. (15), overshooting reaches a slightly higher level in the diffusion models.

Table 4b shows the results for more multi-parcel models based on Eq. (15), bridging lines 3 and 6 of Table 4a. For the last of these, the model with 32 path lengths, Fig. 6 illustrates the variation of ΔT and w for each parcel. As in Fig. 5, the actual position of a parcel is given as the sum of the ordinate (start position) and the upper abscissa. The maximum of ΔT is reached near $\lg P = 4.22$ (slightly *below* the level where $\nabla = \nabla_{\rm ad}$, because of radiative relaxation), and $\Delta T = 0$ occurs near $\lg P = 3.91$ (heavy line in the left panel).

The impact of efficient radiative relaxation on the layer of convective overshooting becomes especially clear with the variation of the scale $l_{\rm opt}$, in relation to the mixing length $l_{\rm mix}$ (Table 4c). The cause is as explained above: with decreasing optical thickness relaxation becomes faster, buoyancy braking becomes less efficient, and thus overshooting can proceed farther.

5.2. Comparison with numerical simulation

We may ask why, in view of existing three-dimensional numerical simulation, one should not abandon mixing-length theory altogether, instead of modifying it by radiative relaxation and arbitrary formalisms that allow for overshooting. However, numerical simulation is either done globally with a rather coarse resolution, or locally in a box that covers only a small fraction of the convection zone; moreover, it is difficult to formulate the correct boundary conditions, in particular for the open boundaries of a box.

Sometime in the future, numerical simulation may indeed replace the mixing-length model. As for now, numerical results may be parameterized in terms of a temperature gradient and in this manner be incorporated into stellar models (Chan & Sofia 1989, Lydon et al. 1992, Lydon et al. 1993). Alternatively, they may be used as a test for mixing-length models such as those described in the present section. To this end we consider the recent 3D simulations of Kim & Chan (1998) and of Stein & Nordlund (1998). In Fig. 7 we show their results, together with results of our models listed in Table 4c. The two simulations cover layers of different extent, and the results are given in terms of different independent variables ($\lg P$ resp. height z above the average photospheric height). Both simulations yield larger downward than upward vertical velocities. For comparison with the r.m.s. velocity of Kim & Chan and

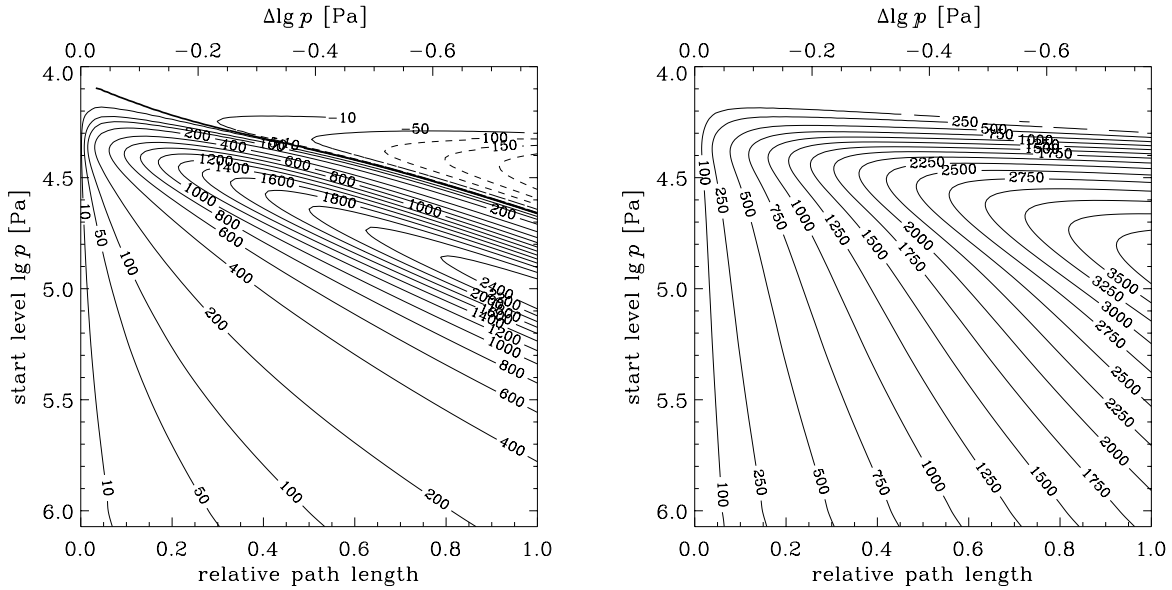

Fig. 6. Temperature excess ΔT (*left*) and vertical velocity w (*right*) of gas parcels along their path towards the upper edge of the convection zone, for a 32-parcel model with $l_{\rm opt}/l_{\rm mix} = 1$. Notation as in Fig. 5.

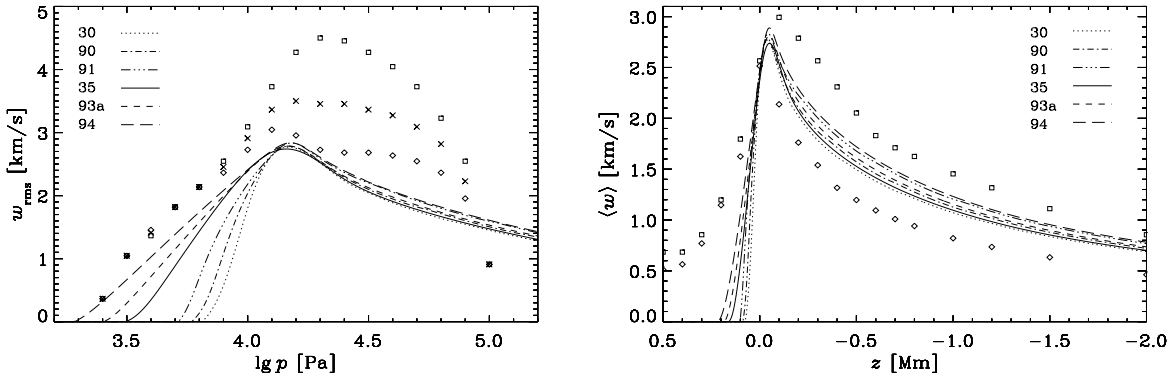

Fig. 7. The vertical velocity in numerical simulations and in mixing-length models with overshooting. Simulation of Kim & Chan (1998 *left*, rms velocity) and Stein & Nordlund (1998 *right*, average velocity): *diamonds* denote upward, *squares* downward, and *crosses* mean velocities. The *lines* represent models of Table 4c, as marked. The scale is as in the respective numerical simulations; notice that the left panel covers a smaller range, only from $z \approx -0.5$ Mm to $z \approx 0.2$ Mm.

the mean velocity of Stein & Nordlund we calculate from our results

$$w_{\rm rms} = \sqrt{\sum_m w_m^2/M}\ , \qquad \langle w \rangle = \sum_m w_m/M\ . \tag{19}$$

Below the surface, i.e. for $z < 0$, our mean velocity falls in the range of $\langle w \rangle$ obtained by Stein and Nordlund, and the velocity maximum occurs approximately at the same level and with the same magnitude as theirs. On the other hand, their simulation predicts substantially farther overshooting than even our model Nr. 94 with $h_{w=0} = 216.5$ km. Here the agreement with the results of Kim & Chan appears to be better; however, their closed boundaries enforce $w = 0$ at the top and at the bottom of their box, which is markedly shallower than the box of Stein & Nordlund.

5.3. Comparison with observation

There are several difficulties connected to the observation of velocity and intensity fluctuations in the solar atmosphere. One is the image degradation caused by the terrestrial atmosphere, which cannot always be corrected reliably because the point-spread function is unknown. Partial solar eclipses have been used to obtain that function; alternatively, observations from above the atmosphere, from the balloon *Spektro-Stratoskop* 28 km above ground, have been used. Another difficulty, especially relevant to the convection studied in the present paper, is the necessity to separate convective from oscillatory fluctuations; such separation is possible if a (k, ω)-diagram is available (Bässgen & Deubner 1982, Espagnet et al. 1995 e.g.), but even then uncertainties remain. In spite of these difficulties there appears to be a clear signature of convective overshooting in the

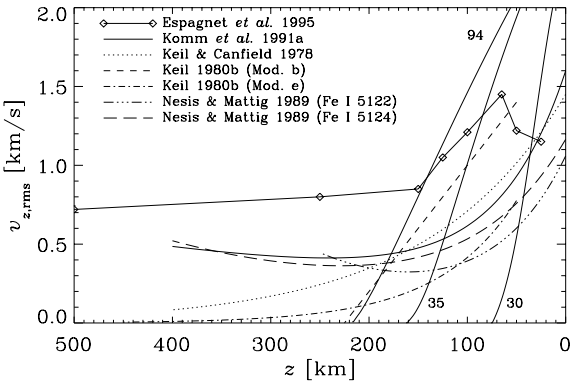

Fig. 8. Observed vertical velocity in the solar atmosphere, and results of three mixing-length models with convective overshooting (Table 4).

height range of the solar atmosphere that is accessible to spectroscopy: velocity fluctuations that are coherent over a rather large distance, but intensity fluctuations loosing their coherence (and their positive correlation to the velocity) already at some intermediate height (Nesis et al. 1988, Nesis & Mattig 1989). The granular vertical r.m.s. velocity at $z = 0$ (mean level of optical depth $\tau = 1$) is in the range 1 – 2 km/s, and decreases with increasing height z; the scale of decrease is of order 150 km (Keil & Canfield 1978, Komm et al. 1990, Komm et al. 1991a, Komm et al. 1991b). The r.m.s. amplitude of the temperature fluctuations at $z = 0$ is 700 K according to Keil & Canfield (1978) and 380 K according to Kneer et al. (1980); the scale of the vertical decrease is only 50 km, or even less.

At greater height granular velocity fluctuations seem to persist coherently, although at small r.m.s. amplitude. Temperature fluctuations also exist at higher levels; their amplitude is small – $\approx$ 75 K according to Kneer et al. (1980) – and they are *anti-correlated* to the velocity at levels above $z \approx 150$ km (Salucci et al. 1994, Rodríguez Hidalgo et al. 1996, Ruiz Cobo et al. 1996).

Some of the observed velocities are shown in Fig. 8. The values of the vertical r.m.s. velocities $v_{z,\mathrm{rms}}$ were taken from figures or tables by Keil & Canfield (1978), Keil (1980a, 1980b), Nesis & Mattig (1989), Komm et al. (1991a), and Espagnet et al. (1995). For comparison, the vertical variation of w in our models Nr. 30, 35, and 94 (Table 4) is also shown. The observational results do not agree well with each other. A possible reason of the spread is the dependence of the vertical variation on the horizontal and time scales of variation, and that the separation of convection and 5-min oscillations in Fourier space has not always been carried out (Nesis & Mattig 1989, Komm et al. 1991a use only a spatial filter with a cut-off at $k = 2.5$ Mm^{-1}). Nevertheless it is conspicuous that in our mixing-length models the velocity decrease with increasing z generally is steeper than observed: the maximum velocity in the deep photosphere is larger, and the extent of the overshooting is less than indicated by all observational results. The model of Ulrich (1976), which operates with radiative relaxation similar to our models, yields such extended overshooting; however, this could be a consequence of the 'diffusion length' of 0.5 to 1.5 pressure scale heights, which he used for vertical smoothing. The origin of the rather large (500 to 800 m/s) velocity in the range above $z = 200$ km in some of the observational studies is not clear; suggestions include plume-like upflows and downflows, shear turbulence, and residual contributions from oscillatory motions.

The level $h_{F_{\mathrm{conv}}=0}$, which should be identified with the level where the correlation between ΔT and w changes into anti-correlation, appears to be higher in the solar atmosphere than predicted by most of the mixing-length models. Deep in the unstable region, at $z \approx -70$ km, a maximum occurs in the convective velocity of all models. This is at optical depth $\tau \approx 10$ and therefore invisible; but Vollmöller et al. (1996) analyzed spectrograms in the range of the opacity minimum around 410 nm and found that the inward increase of v becomes less steep in the deepest accessible layers – possibly an indication of the maximum further down.

In order to compare the *magnitude* of ΔT with observational results, we must recall that the level where $\tau = 1$ is not defined by a fixed value of z but depends on ΔT itself within each parcel. We have calculated that level, using the parcel temperature and density, and the opacity table. The ΔT for the surface $\tau = 1$ obtained in this manner corresponds, by order of magnitude, to the values quoted above; however, the detailed result greatly depends on the location of the characteristic levels h_{cc} and $h_{F_{\mathrm{conv}}=0}$ (Table 4). Model Nr. 93a, with $\Delta T_{\mathrm{rms}} = 273$ K, comes closest to the 360 K of Kneer et al. (1980).

5.4. Stratification and oscillation frequencies

We have already seen (Figs. 3 and 4) that – in case of the standard mixing-length theory – a modification of the radiative relaxation yields a modification of the temperature gradient, and therefore of the temperature in the convection zone itself, with consequences for the p-mode eigenfrequencies. We now find that the effect obtained there becomes less pronounced with the addition of the "non-local" formalism; the effect is even reversed for some of the models. It appears that the "non-local" mixing-length formalism yields a more efficient convective energy transport than the local formalism. Hence the maximum of ∇ is less pronounced, and occurs at a slightly deeper level. Therefore the temperature increase is not as steep as in the local models. In fact only for models Nr. 91 and 94, those with the shortest scale l_{opt}, the temperature of the outer convection zone exceeds that of the reference model STD. Model Nr. 13, with no relaxation (i.e. adiabatic parcels), and model Nr. 17, based on the diffusion approximation, have the highest efficiency of convective transport and hence the smallest maximum value of ∇, at the deepest location. Models Nr. 90 and 93a are intermediate: the effects of radiative relaxation and of multi-parcel convection tend to cancel each other in these models.

The change of p-mode eigenfrequencies for the diverse models corresponds to the change of the temperature profile. Fig. 10 illustrates examples of frequency changes relative to the reference model. In order to understand these results we must realize that the temperature change deeper in the convection zone (to

the right of the range shown in Fig. 9) is opposite to the change just below the surface. The net result is such that only models 91 and 94, in which the radiative effect dominates over the effect on non-local convection, show a normalized frequency decrease of up to several μHz.

6. Conclusions and final remarks

We have presented a modified mixing-length theory of convection which is used to develop a local and a "non-local" formalism. Both versions include a formulation of radiative dissipation which is valid for the optical thick and the optical thin case. Contrary to standard mixing-length theory we allow for different length scales of convection and radiation. The ratio of the radiative to the convective scale is given by the parameter $l_{\rm opt}/l_{\rm mix}$. In the "non-local" version of our formalism we consider a multitude of convective elements with different path lengths. Here the parameter M is introduced which gives the number of convective parcels taken into account.

The initial helium content Y_0 and the mixing-length parameter α are determined as usual by fitting the solar models and envelopes to the current values of radius and luminosity. All other parameters remain free. Consequently we can only use them for a parameter study. The parameter $l_{\rm opt}/l_{\rm mix}$ exerts a strong influence on the stratification of the upper convection zone and on the frequencies of the solar eigenoscillations. This indicates that radiative effects are an essential ingredient of future convection theories. It is not sufficient to have a reasonable scheme for the turbulent convection; equally important is a sound treatment of the radiation field. It is only fair to say that one might not realistically expect more conclusive statements from the mixing-length theory or any formalisms based on it, since this theory is merely a convenient way to overcome our ignorance on stellar convection with the help of a single parameter, namely α.

We want to add some remarks with respect to approximations made within the mixing-length theory in general and in our treatment in special.

One approximation within the mixing-length theory and behind the formula of Spiegel (1957) for the radiative relaxation time is that variations of quantities are small compared to the background. This allows a linearized treatment. An additional approximation is that the convective processes do not disturb the hydrostatic equilibrium and that the radiative processes are quasistatic. These assumptions are no longer valid in the upper convection zone where the temperature variations can reach 30% or more of the mean temperature and where dynamic effects, e.g. the turbulent pressure, become important. From this it becomes clear that we cannot expect to model the stratification of this region with our mixing-length theory with good accuracy. A treatment of higher order including full time dependence would be needed to model the physics more appropriate. Nevertheless the formalisms based on the linearized description can be assumed to give the right order of magnitude and to show the essential dependencies on certain parameters.

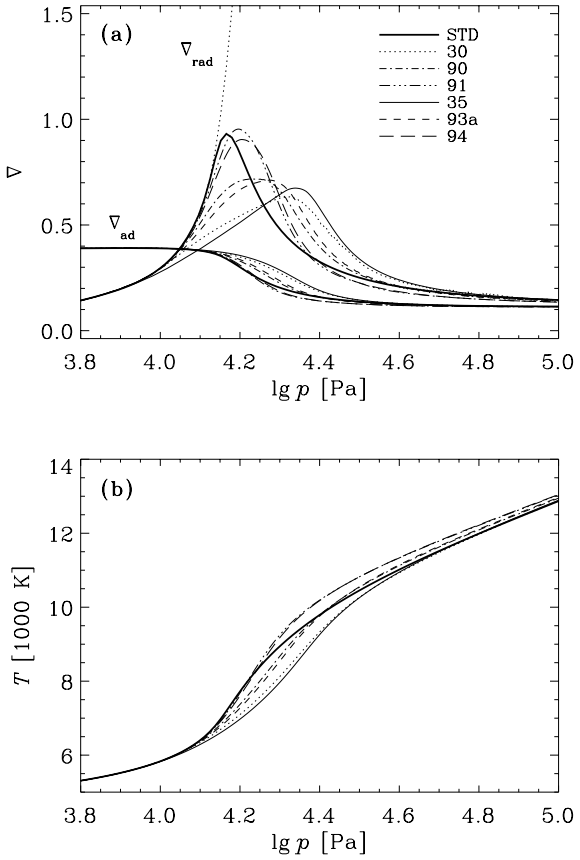

Fig. 9a and b. Temperature gradient ∇ (**a**) and temperature (**b**) in the uppermost part of the convection zone for models based on non-local mixing-length theory with modified radiative relaxation (cf. Table 4).

In general the structure of the convection zone is determined by the requirement that the internally generated energy must be transported outward. The local temperature gradient will take a value as to support that transport. This local adjustment will independently take place at every depth, in the deep convection zone where convection is almost adiabatic as well as in the upper layers where radiative effects play an important role. In the mixing-length theory the variation of the only free parameter α is used to fit the solar model to the Sun. This value of α then determines the run of the temperature gradient in the *entire* convection zone. Now a change in the efficiency of radiative relaxation, e.g. by a decrease of $l_{\rm opt}/l_{\rm mix}$, will strongly affect the convection in the upper part of the convection zone while the influence on its deeper parts should be negligible. Therefore in the fitting procedure the value of α is mainly determined by the convection in the upper convection zone. On the other hand, the overshoot length at the base of the convection zone depends on the mixing-length parameter. Thus we have the unreasonable circumstance that the situation at the top of the convection zone directly rules the properties of the lower convection zone and below. We must conclude once more that more refined theories of compressible turbulent convection should be used if one wants to learn about the overshoot at the base of the solar convection zone. Thus, we concede that the formalisms used in this work

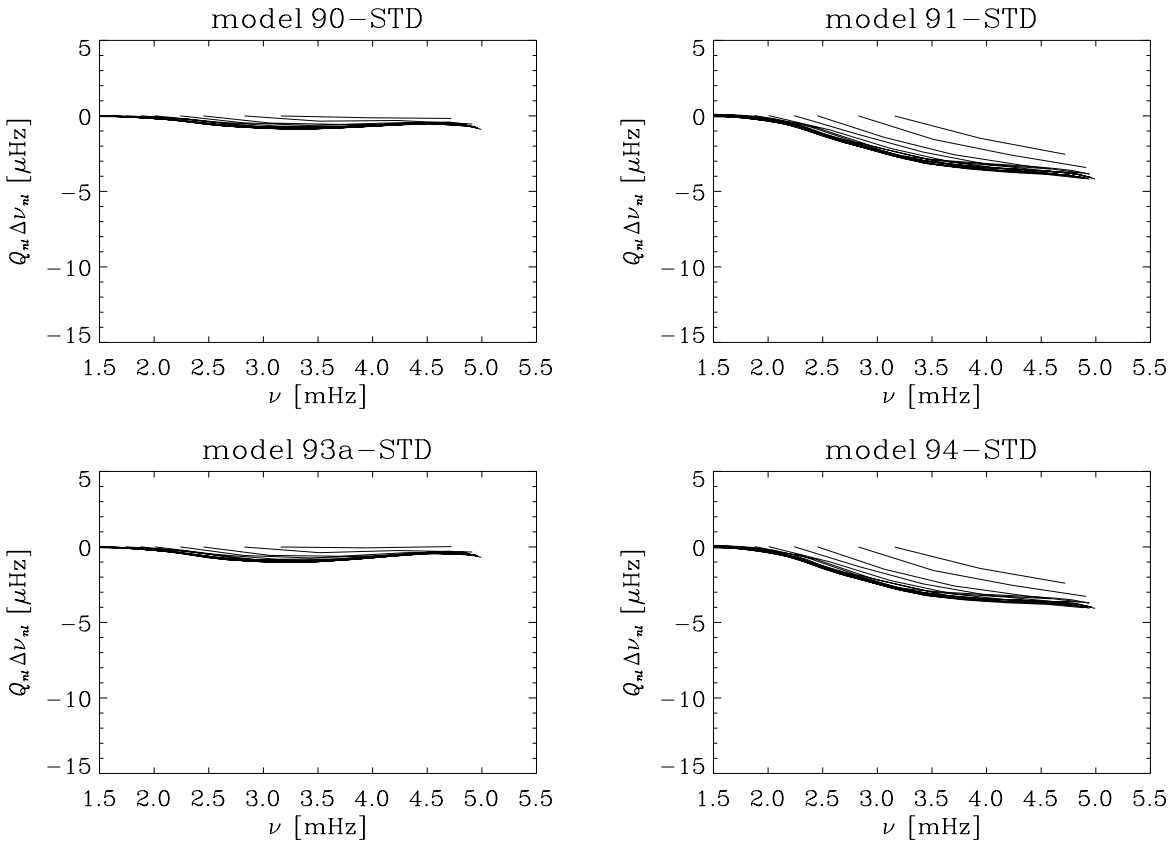

Fig. 10. Frequency changes of four models with non-local mixing-length theory and modified radiative relaxation (cf. Table 4), as compared to model STD. The changes are calculated for the same degrees $l = 0 \ldots 1000$ as in Fig. 2, in ascending order of the curves, and with weights Q_{nl} as in Fig. 2.

have only limited predictive power with respect to the overall properties of the solar convection zone. On the other hand they offer a convenient means to asses dependencies on certain parameters, e.g. on the radiative relaxation. Models of this type might still be useful to test the importance of ingredients in more complicated models of stellar convection.

Acknowledgements. We thank F.J. Rogers and D.R. Alexander for providing their opacity tables, S. Tomczyk for making his LOWL p-mode frequencies available, and A. Nesis for valuable remarks with respect to photospheric observations. Part of this work was supported by the Deutsche Forschungsgemeinschaft.

References

Alexander D.R., Ferguson J.W., 1994, ApJ 437, 879
Bachmann K.T., Duvall T.L., Harvey J.W., Hill F., 1995, ApJ 443, 837
Bässgen M., Deubner F.-L., 1982, A&A 111, L1
Basu S., Antia H.M., Narasimha D., 1994, MNRAS 267, 209
Böhm-Vitense E., 1958, Z. Astrophys. 46, 108
Canuto V.M., Mazzitelli I., 1991, ApJ 370, 295
Canuto V.M., Mazzitelli I., 1992, ApJ 389, 724
Canuto V.M., Goldman I., Mazzitelli I., 1996, ApJ 473, 550
Chan K.L., Sofia S., 1989, ApJ 336, 1022
Christensen-Dalsgaard J., 1994, *Lecture notes on stellar oscillations*, Institut for Fysik og Astronomi, Aarhus Universitet
Christensen-Dalsgaard J., 1997, In: Pijpers F.P., Christensen-Dalsgaard J., Rosenthal C.S. (eds.), *SCORe '96: Solar convection and oscillations and their relationship*, Kluwer Acad. Publishers, p. 3
Christensen-Dalsgaard J., Monteiro M.J.P.F.G., Thompson M.J., 1995, MNRAS 276, 283
Dorfi E.A., Drury L.O'C, 1987, J. Comp. Phys. 69, 175
Espagnet O., Muller R., Roudier Th., Mein N., Mein P., 1995, A&AS 109, 79
Grabowski U., 1996, *Nichtadiabatische Oszillationen der ganzen Sonne*, Dissertation, Univ. Freiburg
Guenther D.B., 1994, ApJ 422, 400
Henyey L.G., Vardya M.S., Bodenheimer P., 1965, ApJ 142, 841
Hummer D.G., Mihalas D., 1988, ApJ 331, 794
Iglesias C.A., Rogers F.J., 1996, ApJ 464, 943
Keil S.L., 1980a, ApJ 237, 1024
Keil S.L., 1980b, ApJ 237, 1035
Keil S.L., Canfield R.C., 1978, A&A 70, 169
Kiefer M., 1999, *Der Einfluß von Konvektion auf die Oszillationen der Sonne*, Dissertation, Univ. Freiburg
Kiefer M., Grabowski U., Stix M., 1996, In: Noels A., Fraipont-Caro D., Gabriel M., Grevesse N., Demarque P. (eds.), *Stellar Evolution: What should be done?* 32nd Liège Int. Astrophys. Coll., Univ. de Liège, p. 379
Kim Y.C., Chan K.L., 1998, ApJ 496, L121
Kneer F., Mattig W., Nesis A., Werner W., 1980, Solar Phys. 68, 31
Komm R., Mattig W., Nesis A., 1990, A&A 239, 340
Komm R., Mattig W., Nesis A., 1991a, A&A 243, 251

Komm R., Mattig W., Nesis A., 1991b, A&A 252, 812
Libbrecht K.G., Woodard M.F., Kaufman J.M., 1990, ApJS 74, 1129
Lydon T.J., Fox P.A., Sofia S., 1992, ApJ 397, 701
Lydon T.J., Fox P.A., Sofia S., 1993, ApJ 403, L79
Mihalas D., Däppen W., Hummer D.G., 1988, ApJ 331, 815
Monteiro M.J.P.F.G., Christensen-Dalsgaard J., Thompson M.J., 1994, A&A 283, 247
Nesis A., Mattig W., 1989, A&A 221, 130
Nesis A., Durrant C.J., Mattig W., 1988, A&A 201, 153
Paternò L., Ventura R., Canuto V.M., Mazzitelli I., 1993, ApJ 402, 733
Pidatella R.M., Stix M., 1986, A&A 157, 338
Renzini A., 1987, A&A 188, 49
Rodríguez Hidalgo I., Ruiz Cobo B., del Toro Iniesta J.C., Collados M., Sánchez Almeida J., 1996, In: Saniga M. (ed.), JOSO Ann. Rep. 1995, p. 162
Rosenthal C.S., Christensen-Dalsgaard J., Houdek G., Monteiro M.J.P.F.G., Nordlund Å., Trampedach R., 1995, In: Hoeksema J.T., Domingo V., Fleck B., Battrick B. (eds.), *Fourth SOHO Workshop, Helioseimology*, ESA SP-376, p. 459
Rosenthal C.S., Christensen-Dalsgaard J., Nordlund Å, Stein R.F., Trampedach R., 1999, A&A 351, 689
Ruiz Cobo B., del Toro Iniesta J.C., Rodríguez Hidalgo I., Collados M., Sánchez Almeida J., 1996, In: Pallavicini R., Dupree A.K. (eds.), ASP Conf. Ser. 109, 155
Salucci G., Bertello L., Cevallini F., Ceppatelli G., Righini A., 1994, A&A 285, 322
Shaviv G., Salpeter E.E., 1973, ApJ 184, 191
Skaley D., Stix M., 1991, A&A 241, 227
Spiegel E.A., 1957, ApJ 126, 202
Spiegel E.A., 1963, ApJ 138, 216
Stein R.F., Nordlund Å., 1998, ApJ 499, 914
Stix M., 1989, *The Sun*, Springer, Berlin Heidelberg
Stix M., Kiefer M., 1997, In: Pijpers F.P., Christensen-Dalsgaard J., Rosenthal C.S. (eds.), *SCORe '96: Solar convection and oscillations and their relationship*, Kluwer Acad. Publishers, p. 69
Stix M., Zhugzhda Y.D., 1998, A&A 335, 685
Thompson J.F., Warsi Z.U.A., Mastin C.W., 1985, *Numerical Grid Generation*, North-Holland, New York Amsterdam Oxford
Tomczyk S., Streander K., Card G., Elmore D., Cacciani A., 1995, Solar Phys. 159, 1
Ulrich R.K., 1970a, Ap&SS 7, 71
Ulrich R.K., 1970b, Ap&SS 7, 183
Ulrich R.K., 1976, ApJ 207, 564
Unsöld A., 1930, Z. Astrophys. 1, 138
Vollmöller P., Komm R., Mattig W., 1996, A&A 306, 294
Zhugzhda Y.D., Stix M., 1994, A&A, 291, 310